



Synthesis and evaluation of chromone-2-carboxamido-alkylamines as potent acetylcholinesterase inhibitors

Paptawan Suwanhom¹ · Teerapat Nualnoi² · Pasarat Khongkow³ · Vannajan Sanghiran Lee⁴ · Luelak Lomlim¹

Received: 1 August 2019 / Accepted: 13 January 2020
© Springer Science+Business Media, LLC, part of Springer Nature 2020

Abstract

Alzheimer's disease (AD) is considered one of the greatest global public burdens. Pathophysiology of AD is proposed to be associated with reduced levels of the neurotransmitter acetylcholine (ACh). Cholinesterase enzymes, namely acetylcholinesterase (AChE) and butyrylcholinesterase (BChE) cleave ACh via hydrolysis. Cholinesterase inhibitors (ChEIs) are the main group of drugs currently used for the treatment of AD. Novel chromone-2-carboxamido-alkylamines (**7–18**) were designed, synthesized, and evaluated for cholinesterase inhibitory activity. The compounds exhibited potent AChE inhibitory activities at micromolar range (IC_{50} 0.09–9.16 μ M) and demonstrated weak BChE inhibitory activities (IC_{50} 12.09–44.56 μ M). Compound **14** (IC_{50} 0.09 ± 0.02 μ M) was the most potent AChEI in this series; it showed higher activity than the clinical used drug tacrine. Enzyme kinetic study suggested that **14** was an uncompetitive inhibitor. Molecular docking study revealed that **14** was a dual-binding site inhibitor. Compound **14** did not induce any concentration-related cytotoxic effect against SH-SY5Y cells. It also showed neuroprotective effect in the cell line. Chromone-2-carboxamido-alkylamines can be promising lead compounds for development of anti-Alzheimer's agents.

Keywords Chromone · Acetylcholinesterase inhibitors · Neuroprotective · Molecular docking

Introduction

Alzheimer's disease (AD) is a neurodegenerative disorder characterized by progressive memory loss and personality change (Mayeux and Sano 1999). AD is considered one of the greatest global public burdens, currently affecting more than 46 million people worldwide (Yiannopoulou and

Papageorgiou 2013). As the average lifespan of the global population increases, neurodegenerative diseases become more prevalent. Pathogenesis of AD is still unclear. Low levels of acetylcholine (ACh) in various regions in the brain, β -amyloid aggregation (Hardy and Selkoe 2002) and oxidative stress are proposed to be key factors in AD pathophysiology (Baptista et al. 2014; Tang and Kumar 2008).

Drug therapy of AD mainly depends on acetylcholinesterase inhibitors (AChEIs) such as tacrine (Ahmed et al. 2006), galanthamine (Greenblatt et al. 1999), donepezil (Sugimoto et al. 2000), and rivastigmine. These drugs increase ACh levels at cholinergic brain synapses through inhibition of the ACh degrading enzyme, AChE (Mehta et al. 2012). AChE resides in the serine protease family. X-ray crystallographic analysis of AChE from *Torpedo californica* (TcAChE) revealed the active site of the enzyme as a narrow, 20 Å deep gorge. Several aromatic amino acids lining the entrance of the gorge form the "peripheral anionic site" (PAS). The catalytic triad that functions in ACh hydrolysis is located at the bottom of the narrow gorge. "Catalytic anionic site" (CAS) and acyl pocket support ACh binding during the hydrolytic degradation process (Bourne et al. 1995; Chatonnet and Lockridge 1989). Several AChEIs exert their activity via binding at CAS or both CAS and PAS sites, as so called

Supplementary information The online version of this article (<https://doi.org/10.1007/s00044-020-02508-5>) contains supplementary material, which is available to authorized users.

✉ Luelak Lomlim
luelak.l@psu.ac.th

- ¹ Department of Pharmaceutical Chemistry, Faculty of Pharmaceutical Sciences, Prince of Songkla University, Hat Yai, Songkhla 90112, Thailand
- ² Department of Pharmaceutical Technology, Faculty of Pharmaceutical Sciences, Prince of Songkla University, Hat Yai, Songkhla 90112, Thailand
- ³ Institute of Biomedical Engineering, Faculty of Medicine, Prince of Songkla University, Hat Yai, Songkhla 90112, Thailand
- ⁴ Department of Chemistry, Faculty of Science, University of Malaya, 50603 Kuala Lumpur, Malaysia

“dual-binding site inhibitors” and block the hydrolysis of ACh. While tacrine and galanthamine have high affinity toward the CAS, donepezil acts as a dual-binding site inhibitor and leads to higher potency and selectivity for AChE (Castro and Martinez 2001).

Chromone is a scaffold that has attracted much attention due to diverse biological properties such as anti-inflammatory, metal chelating and neuroprotective effects (Grazul and Budzisz 2009). Mimicking the indanone ring (red) of donepezil, chromone moiety (red) was used as a scaffold for the design of the target compounds. Several reported AChEIs contain at least one basic amino group in their molecular structure, either in the form of *N*-aryl or *N*-aralkyl moieties. In physiological pH, the protonated amino group binds with aromatic amino acid residues at the CAS via cation- π interaction. The aromatic residue in *N*-aryl or *N*-aralkyl moieties was predicted to form π - π interaction in the CAS region and supported the binding of the molecule to the active site gorge of the enzyme (Liu et al. 2015). However, *N*-aryl or *N*-aralkyl moieties were not found to be essential for AChE inhibitory activity. Some AChEIs bearing chromone moiety with side chains containing *N*-alkyl or alicyclic amine also exhibited potent AChE inhibitory activity (Sang et al. 2017); (Pourshojaei et al. 2015; Luo et al. 2016). These findings inspired us to design new chromone-2-carboxamido-alkylamines as AChEIs using chromone as a PAS binding unit (red). Piperidine ring or dimethylamine moieties bearing a tertiary amino group (blue) were incorporated in the structure. These amine moieties were anticipated to bind with the CAS. The chromone and tertiary amino groups were connected via a methylene chain with various lengths ($n = 2, 3$) in order to explore the optimal distance between the two units. As the structure of donepezil consists of a dimethoxyl indanone ring, positions 6- and 7- of the chromone ring system of our designed compounds were replaced with mono- or dimethoxyl groups to explore structure-activity relationships. Figure 1 illustrates the idea in the design of the chromone-2-carboxamido-alkylamines in this work.

BChE is also able to hydrolyze ACh and is known as pseudocholinesterase. This enzyme is found primarily in the liver, intestine, heart, lung, and the brain (Cokugas 2003). In a normal human brain, AChE accounts for major cholinesterase activity. There is growing evidence that both AChE and BChE may be important in the development and progression

of AD. Up to 45% of AChE may be lost in certain brain regions during progression of AD while levels of BChE activity conversely increase by up to 90%. Thus, both enzymes have been identified as potential targets in the treatment of AD (Greig et al. 2002). In this research, we describe design, synthesis, and evaluation of AChE and BChE inhibitory activities of chromone-2-carboxamido-alkylamine derivatives. The mode of AChE inhibition was explored. Molecular docking was employed to predict interactions between the inhibitor and the enzymes. Cytotoxicity of the synthesized compounds was evaluated in SH-SY5Y cells.

Materials and methods

Experimental

All chemical and solvents required for synthesis were purchased from Sigma-Aldrich. All reaction was checked by thin layer chromatography and visualized by UV light. Column chromatography was performed on silica gel. IR spectra were performed on a Perkin Elmer spectrum and principal absorptions were given in cm^{-1} . $^1\text{H-NMR}$ and $^{13}\text{C-NMR}$ spectra were measured on a Varian Unity Inova 500 MHz. NMR spectrometer using deuterated chloroform (CDCl_3) or dimethylsulfoxide (d_6 -DMSO) as solvent. The coupling constants are reported in Hertz (Hz). Proton coupling patterns were designed as s, singlet; d, doublet; t, triplet; m, multiplet. Melting points were recorded using the Mel-TEMP II LABORATORY DEVICES, USA. ESI-MS spectra were recorded on a Thermo Finnigan MAT 95XL. The Power Wave x, Biotele was used as a microplate reader.

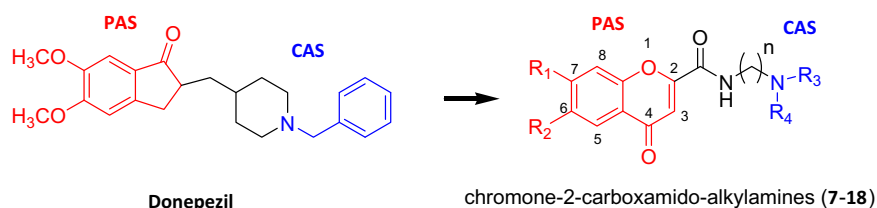
Chemistry

Pathway for the synthesis of the desired chromone-2-carboxamido-alkylamines can be illustrated in Scheme 1.

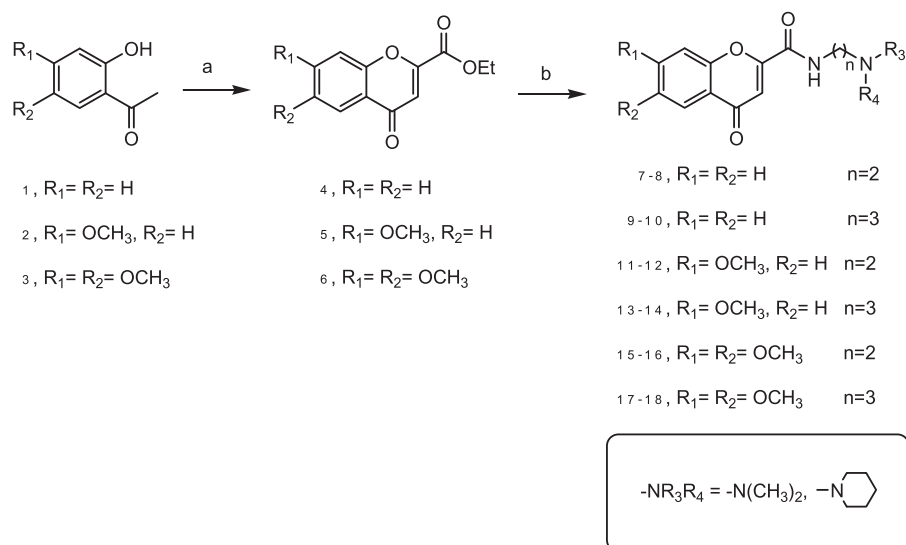
General procedure for the preparation of compounds 4–6

Sodium hydride (65 mmol) was dissolved in tetrahydrofuran (THF, 10 ml) and then diethyl oxalate (35 mmol) solution in THF (20 ml) was added. The reaction mixture was stirred overnight at room temperature under

Fig. 1 Design strategy of chromone derivatives



Scheme 1 Synthesis of chromone derivatives: (a) diethyl oxalate, NaH/THF, room temperature; (b) amine/CH₂Cl₂/reflux, then CH₃COOH, 70 °C



nitrogen. It was then poured into iced-water (70 ml), HCl (6 N, 20 ml), and extracted with diethylether (3 × 80 ml). The precipitated solid was dried in a vacuum to give a yellow solid. The product was purified by chromatography on the silica gel by using ethyl acetate:hexane (40:60) as mobile phase and then recrystallized in ethyl acetate to give ethyl-4-oxo-4*H*-chromene-2-carboxylate (**4**–**6**).

Ethyl-4-oxo-4*H*-chromene-2-carboxylate (4) Pale yellow solid (82% yield), m.p. 100–102 °C; IR (KBr): ν (cm⁻¹) 3448, 2984, 1740, 1658, 1465, 1258, and 772. ¹H-NMR (DMSO-*d*₆, 500 MHz) 1.32 (t, *J* = 7.11 Hz, 3H), 4.37 (q, *J* = 7.11 Hz, 2H), 6.92 (s, 1H), 7.51 (ddd, *J* = 1.04, 7.15, 8.11 Hz, 1H), 7.71 (m, 1H), 7.85 (ddd, *J* = 1.72, 7.15, 8.57 Hz, 1H), and 8.02 (dd, *J* = 1.59, 8.11 Hz, 1H). ¹³C-NMR (DMSO-*d*₆, 125 MHz) 14.03, 62.87, 113.91, 119.04, 123.94, 125.12, 126.38, 135.49, 152.44, 160.15, and 177.54.

Ethyl-7-methoxy-4-oxo-4*H*-chromene-2-carboxylate (5) Pale yellow solid (78% yield), m.p. 113–115 °C; IR (KBr): ν (cm⁻¹) 3462, 2919, 1743, 1439, 1257, and 778. ¹H-NMR (DMSO-*d*₆, 500 MHz) 1.34 (t, *J* = 7.11 Hz, 3H), 3.92 (s, 3H), 4.39 (quin, *J* = 7.11 Hz, 2H), 6.88 (s, 1H), 7.10 (dd, *J* = 2.40, 8.88 Hz, 1H), 7.23 (d, *J* = 2.39 Hz, 1H), and 7.94 (d, *J* = 8.88 Hz, 1H). ¹³C-NMR (DMSO-*d*₆, 125 MHz) 14.04, 56.49, 62.79, 101.16, 114.12, 115.90, 117.83, 126.53, 152.11, 157.51, 160.15, 164.81, and 176.48.

Ethyl-6,7-dimethoxy-4-oxo-4*H*-chromene-2-carboxylate (6) Pale yellow solid (86% yield), m.p. 116–117 °C; IR (KBr): ν (cm⁻¹) 3606, 2983, 1742, 1632, 1510, 1255, and 865. ¹H-NMR (DMSO-*d*₆, 500 MHz) 1.34 (t, *J* = 7.11 Hz, 3H), 3.86 (s, 3H), 3.94 (s, 3H), 4.39 (quin, *J* = 7.11 Hz, 2H), 6.89 (s, 1H), 7.29 (s, 1H), 7.35 (s, 1H). ¹³C-NMR

(DMSO-*d*₆, 125 MHz) 14.38, 56.35, 57.11, 63.04, 101.31, 103.90, 113.79, 117.73, 148.51, 151.99, 152.07, 155.69, 160.52, and 176.39.

General procedure for the preparation of compounds 7–18

Ethyl-4-oxo-4*H*-chromene-2-carboxylate derivatives (**4**–**6**, 0.46 mmol) and *N,N*-dimethylenediamine (1.38 mmol) were dissolved in dichloromethane (5 ml), added to a round bottom flask and allowed to reflux for 20 min. Then, glacial acetic acid (5 ml) was added and the solution was stirred at 75 °C under a nitrogen atmosphere for 24 h. The mixture was extracted with ethyl acetate (3 × 80 ml). The organic layer was dried by vacuum. The product was purified by chromatography on the silica gel by using dichloromethane:methanol (80:20) as mobile phase and then recrystallized in ethyl acetate to give chromone-2-carboxamido-alkylamine derivatives (**7**–**18**)

***N*-(2-(dimethylamino)ethyl)-4-oxo-4*H*-chromene-2-carboxamide (7)** Yellow liquid (64% yield), 100% HPLC purity, m.p. 97–100 °C; IR (KBr): ν (cm⁻¹) 3851, 3311, 2947, 1652, 1532, 1464, 1387, 1018, and 758. ¹H-NMR (DMSO-*d*₆, 500 MHz) 2.21 (s, 6H), 2.48 (m, 2H), 3.39 (m, 2H), 6.81 (s, 1H), 7.53 (m, 1H), 7.72 (m, 1H), 7.88 (ddd, *J* = 1.72, 7.11, 8.50 Hz, 1H), 8.04 (dd, *J* = 1.89, 7.83 Hz, 1H), and 9.03 (t, *J* = 5.51 Hz, 1H). ¹³C-NMR (DMSO-*d*₆, 125 MHz) 34.40, 45.20, 57.79, 110.57, 118.89, 123.70, 124.98, 126.14, 135.03, 155.20, 155.76, 159.06, and 177.42. ESI-MS: (m/z, [M+H]⁺) (Calcd: 261.1236. Found: 261.1234).

4-oxo-*N*-(2-(piperidin-1-yl)ethyl)-4*H*-chromene-2-carboxamide (8) Pale yellow solid (62% yield), 100% HPLC purity, m.p. 110–113 °C; IR (KBr): ν (cm⁻¹) 3518, 3303, 2936, 1654, 1464, 1385, 1130, and 757. ¹H-NMR (DMSO-*d*₆,

500 MHz) 1.51 (m, 6H), 2.68 (m, 6H), 3.50 (m, 2H), 6.83 (s, 1H), 7.53 (ddd, $J = 1.06, 7.16, 8.07$ Hz, 1H), 7.74 (dd, $J = 0.60, 8.62$ Hz, 1H), 7.88 (ddd, $J = 1.71, 7.16, 8.62$ Hz, 1H), 8.04 (dd, $J = 1.54, 8.07$ Hz, 1H), and 9.21 (s, 1H). ^{13}C -NMR (DMSO- d_6 , 125 MHz) 24.27, 25.82, 37.18, 54.36, 57.45, 110.90, 119.19, 124.11, 125.43, 126.50, 135.48, 155.52, 156.09, 159.42, and 177.75. ESI-MS: (m/z, $[\text{M}+\text{H}]^+$) (Calcd: 301.1549. Found: 301.1547).

N-(3-(dimethylamino)propyl)-4-oxo-4H-chromene-2-carboxamide (9) Pale yellow solid (68% yield), 100% HPLC purity, m.p. 99–112 °C; IR (KBr): ν (cm^{-1}) 3867, 3400, 2943, 1654, 1532, 1464, 1386, 1019, and 758. ^1H -NMR (DMSO- d_6 , 500 MHz) 1.69 (quin, $J = 6.95$ Hz, 2H), 2.16 (s, 6H), 2.30 (t, $J = 6.90$ Hz, 2H), 3.30 (m, 2H), 6.81 (s, 1H), 7.53 (m, 1H), 7.71 (ddd, $J = 0.45, 1.04, 8.48$ Hz, 1H), 7.89 (ddd, $J = 1.73, 7.12, 8.48$ Hz, 1H), 8.05 (dd, $J = 1.70, 7.94$ Hz, 1H), and 9.22 (t, $J = 5.55$ Hz, 1H). ^{13}C -NMR (DMSO- d_6 , 125 MHz) 26.92, 38.50, 45.54, 57.35, 110.79, 119.16, 124.08, 125.40, 126.46, 135.46, 155.52, 156.20, 159.25, and 177.76. ESI-MS: (m/z, $[\text{M}+\text{H}]^+$) (Calcd: 275.1398. Found: 275.1383).

4-oxo-N-(3-(piperidin-1-yl)propyl)-4H-chromene-2-carboxamide (10) Pale yellow solid (63% yield), 100% HPLC purity, m.p. 108–112 °C; IR (KBr): ν (cm^{-1}) 3748, 3429, 2947, 1652, 1606, 1464, 1388, 1019, and 758. ^1H -NMR (DMSO- d_6 , 500 MHz) 1.67 (m, 6H), 1.99 (m, 2H), 2.99 (m, 4H), 3.30 (m, 4H), 6.84 (s, 1H), 7.54 (ddd, $J = 1.04, 7.20, 8.01$ Hz, 1H), 7.75 (dd, $J = 0.49, 8.60$ Hz, 1H), 7.90 (ddd, $J = 1.71, 7.20, 8.60$ Hz, 1H), 8.05 (dd, $J = 1.67, 8.01$ Hz, 1H), and 9.34 (t, $J = 6.06$ Hz, 1H). ^{13}C -NMR (DMSO- d_6 , 125 MHz) 21.57, 22.52, 23.48, 36.82, 52.11, 53.77, 110.62, 118.99, 123.77, 125.08, 126.22, 135.17, 155.25, 155.69, 159.39, and 177.50. ESI-MS: (m/z, $[\text{M}+\text{H}]^+$) (Calcd: 315.1560. Found: 315.1558).

N-(2-(dimethylamino)ethyl)-7-methoxy-4-oxo-4H-chromene-2-carboxamide (11) Pale yellow solid (74% yield), 100% HPLC purity, m.p. 117–119 °C; IR (KBr): ν (cm^{-1}) 3315, 2947, 2823, 1649, 1609, 1439, 1386, 1022, and 833. ^1H -NMR (DMSO- d_6 , 500 MHz) 2.25 (s, 6H), 2.52 (m, 2H), 3.41 (m, 2H), 3.91 (s, 3H), 6.74 (s, 1H), 7.10 (dd, $J = 2.43, 8.88$ Hz, 1H), 7.17 (d, $J = 2.43$ Hz, 1H), 7.94 (d, $J = 8.88$ Hz, 1H), and 9.01 (t, $J = 5.47$ Hz, 1H). ^{13}C -NMR (DMSO- d_6 , 125 MHz) 36.71, 44.61, 56.58, 57.38, 101.38, 111.01, 115.82, 117.86, 126.91, 155.62, 157.36, 159.77, 164.81, and 177.04. ESI-MS: (m/z, $[\text{M}+\text{H}]^+$) (Calcd: 291.1351. Found: 291.1338).

7-methoxy-4-oxo-N-(2-(piperidin-1-yl)ethyl)-4H-chromene-2-carboxamide (12) Pale yellow solid (66% yield), 100% HPLC purity, m.p. 119–121 °C; IR (KBr): ν (cm^{-1}) 3323,

2936, 2839, 1649, 1609, 1439, 1386, 1024, and 835. ^1H -NMR (DMSO- d_6 , 500 MHz) 1.45 (m, 6H), 2.53 (m, 6H), 3.43 (m, 2H), 3.91 (s, 3H), 6.74 (s, 1H), 7.11 (dd, $J = 2.41, 8.87$ Hz, 1H), 7.16 (d, $J = 2.41$ Hz, 1H), 7.94 (d, $J = 8.87$ Hz, 1H), and 9.01 (t, $J = 5.60$ Hz, 1H). ^{13}C -NMR (DMSO- d_6 , 125 MHz) 23.97, 25.43, 36.85, 54.17, 56.54, 57.29, 101.34, 110.95, 115.71, 117.94, 126.86, 155.69, 157.35, 159.47, 172.48, and 176.87. ESI-MS: (m/z, $[\text{M}+\text{H}]^+$) (Calcd: 331.1666. Found: 331.1644).

N-(3-(dimethylamino)propyl)-7-methoxy-4-oxo-4H-chromene-2-carboxamide (13) Pale yellow solid (72% yield), 100% HPLC purity, m.p. 120–123 °C; IR (KBr): ν (cm^{-1}) 3447, 2943, 2863, 1649, 1613, 1440, 1388, 1021, and 836. ^1H -NMR (DMSO- d_6 , 500 MHz) 1.68 (m, 2H), 2.14 (s, 6H), 2.27 (t, $J = 6.95$ Hz, 2H), 2.49 (m, 2H), 3.92 (s, 3H), 6.73 (s, 1H), 7.11 (dd, $J = 2.41, 8.86$ Hz, 1H), 7.15 (d, $J = 2.41$ Hz, 1H), 7.94 (d, $J = 8.86$ Hz, 1H), and 9.13 (t, $J = 4.51$ Hz, 1H). ^{13}C -NMR (DMSO- d_6 , 125 MHz) 26.80, 38.05, 45.28, 56.23, 56.96, 100.98, 110.53, 115.41, 117.63, 126.56, 155.55, 157.06, 158.95, 164.38, and 176.55. ESI-MS: (m/z, $[\text{M}+\text{H}]^+$) (Calcd: 305.1509. Found: 305.1496).

7-methoxy-4-oxo-N-(3-(piperidin-1-yl)propyl)-4H-chromene-2-carboxamide (14) Pale yellow solid (71% yield), 100% HPLC purity, m.p. 123–126 °C; IR (KBr): ν (cm^{-1}) 3421, 2945, 2686, 1650, 1609, 1439, 1386, 1022, and 839. ^1H -NMR (DMSO- d_6 , 500 MHz) 1.89 (m, 8H), 2.66 (m, 6H), 3.35 (m, 2H), 3.91 (s, 3H), 6.76 (s, 1H), 7.11 (dd, $J = 2.42, 8.88$ Hz, 1H), 7.20 (d, $J = 2.42$ Hz, 1H), 7.95 (d, $J = 8.88$ Hz, 1H), and 9.25 (t, $J = 5.77$ Hz, 1H). ^{13}C -NMR (DMSO- d_6 , 125 MHz) 21.83, 22.83, 23.75, 36.97, 52.31, 54.07, 56.27, 101.18, 110.65, 115.41, 117.64, 126.55, 155.35, 157.09, 159.34, 164.41, and 176.60. ESI-MS: (m/z, $[\text{M}+\text{H}]^+$) (Calcd: 345.1823. Found: 345.1804).

N-(2-(dimethylamino)ethyl)-6,7-dimethoxy-4-oxo-4H-chromene-2-carboxamide (15) Pale yellow solid (64% yield), 100% HPLC purity, m.p. 115–118 °C; IR (KBr): ν (cm^{-1}) 3446, 2923, 2863, 1642, 1598, 1536, 1273, 1021, and 863. ^1H -NMR (DMSO- d_6 , 500 MHz) 2.22 (s, 6H), 2.50 (m, 2H), 3.41 (m, 2H), 3.86 (s, 3H), 3.93 (s, 3H), 6.75 (s, 1H), 7.23 (s, 1H), 7.34 (s, 1H), and 9.00 (t, $J = 5.68$ Hz, 1H). ^{13}C -NMR (DMSO- d_6 , 125 MHz) 37.70, 45.55, 56.27–56.75, 58.22, 100.95, 103.96, 110.37, 117.40, 148.24, 151.51, 155.21, 155.32, 159.46, and 176.52. ESI-MS: (m/z, $[\text{M}+\text{H}]^+$) (Calcd: 321.1456. Found: 321.1450).

6,7-dimethoxy-4-oxo-N-(2-(piperidin-1-yl)ethyl)-4H-chromene-2-carboxamide (16) Pale yellow solid (78% yield), 100% HPLC purity, m.p. 121–123 °C; IR (KBr): ν (cm^{-1}) 3422, 2935, 2863, 1643, 1608, 1506, 1270, 1019, and 828. ^1H -NMR (DMSO- d_6 , 500 MHz) 1.49 (m, 6H), 2.58 (m,

6H), 3.46 (m, 2H), 3.86 (s, 3H), 3.93 (s, 3H), 6.76 (s, 1H), 7.23 (s, 1H), 7.34 (s, 1H), and 9.09 (s, 1H). ^{13}C -NMR (DMSO- d_6 , 125 MHz) 23.65, 25.03, 36.46, 53.97, 56.74, 57.09, 100.95, 103.94, 110.34, 117.40, 148.25, 151.51, 155.21, 159.60, 172.51, and 176.52. ESI-MS: (m/z, $[\text{M}+\text{H}]^+$) (Calcd: 361.1763. Found: 361.1754).

N-(3-(dimethylamino)propyl)-6,7-dimethoxy-4-oxo-4H-chromene-2-carboxamide (17) Pale yellow solid (67% yield), 100% HPLC purity, m.p. 119–123 °C; IR (KBr): ν (cm^{-1}) 3447, 2955, 2714, 1643, 1600, 1510, 1275, 1021, and 865. ^1H -NMR (DMSO- d_6 , 500 MHz) 1.90 (m, 2H), 2.70 (s, 6H), 3.02 (m, 2H), 3.35 (m, 2H), 3.87 (s, 3H), 3.94 (s, 3H), 6.77 (s, 1H), 7.22 (s, 1H), 7.36 (s, 1H), and 9.20 (t, $J = 5.84$ Hz, 1H). ^{13}C -NMR (DMSO- d_6 , 125 MHz) 24.67, 36.88, 42.82, 55.11, 56.35–56.82, 100.92, 104.02, 110.44, 117.43, 148.34, 151.56, 155.25, 155.33, 159.89, and 176.58. ESI-MS: (m/z, $[\text{M}+\text{H}]^+$) (Calcd: 335.1615. Found: 335.1605).

6,7-dimethoxy-4-oxo-N-(3-(piperidin-1-yl)propyl)-4H-chromene-2-carboxamide (18) Pale yellow solid (70% yield), 100% HPLC purity, m.p. 122–125 °C; IR (KBr): ν (cm^{-1}) 3423, 2939, 2871, 1643, 1606, 1474, 1276, 1013, and 826. ^1H -NMR (DMSO- d_6 , 500 MHz) 1.80 (m, 8H), 2.94 (m, 6H), 3.35 (m, 2H), 3.12 (s, 3H), 3.93 (s, 3H), 6.77 (s, 1H), 7.23 (s, 1H), 7.35 (s, 1H), and 9.20 (s, 1H). ^{13}C -NMR (DMSO- d_6 , 125 MHz) 21.55, 22.95, 23.97, 36.92, 52.60, 54.18, 56.26–56.75, 100.82, 103.89, 110.36, 117.30, 148.27, 151.51, 155.15, 155.30, 159.88, and 176.64. ESI-MS: (m/z, $[\text{M}+\text{H}]^+$) (Calcd: 375.1934. Found: 375.1915).

Enzyme inhibition assay

AChE and BChE activities were measured by Ellman's method (Ellman et al. 1961) with slight modification. We used AChE both from a human source (*HuAChE*) and an electric eel (*eeAChE*) and BChE from horse serum. The 5,5'-dithiobis-(2-nitrobenzoic acid) (Ellman's reagent, DTNB), acetylthiocholine iodide (ATCI) and butyrylthiocholine iodide (BTCI) were acquired from Sigma-Aldrich.

All the *in vitro* AChE assays were carried out on a 96-well plate. Overall, 25 μL of 100 μM sample was dissolved in ethanol, 125 μL of 3 mM DTNB, 25 μL of 1.5 mM of ATCI, an analog substrate of ACh, 50 μL of 50 mM Tris/HCl (pH = 8), and followed by 25 μL of enzyme. This reaction resulted in the development of a yellow color. The color of the product was measured at 405 nm every 11 s for 2 min. Each experiment was repeated in triplicate. The result of the measurements showed mean velocity which was obtained from graphs plotted between times and absorbance. The percentage of AChE inhibitory activity

(%Inhibition) was calculated by the following expression:

$$\%Inhibition = \frac{(\text{Mean velocity of blank} - \text{Mean velocity of sample}) \times 100}{\text{Mean velocity of blank}}$$

Determination of 50% inhibition of the AChE activity (IC_{50}) values was performed graphically from an inhibition curve (log inhibitor concentration vs. percent of inhibition) and done under the same protocol as above. Eight difference concentrations of the inhibitor ($50 - 1.6 \times 10^{-3} \mu\text{M}$) were used. The response curve was created using Graphpad Prism 2.01.

Enzyme from *horse serum* was used in the *in vitro* BChE assay and BTCI was used as a substrate. This assay was performed using a method similar to that described above. Donepezil and tacrine were used as positive controls. Selectivity of acetylcholinesterase inhibitory activity of the compounds can be evaluated by the ratio between IC_{50} of horse BChE with IC_{50} of *eeAChE* and shown as Selectivity index (SI) (Liston et al. 2004; Rogers and Friedhoff 1998).

Kinetic study

The kinetic study for the characterization of AChE inhibition was evaluated with the same protocol of inhibitory activity by using AChE from an electric eel (Nochi et al. 1995); (Kamal et al. 2000). In this study, compound **14** had the highest inhibitory activity and was chosen. The assay solution (250 μL) consists of 125 μL of 3 mM DTNB, 25 μL of 1.5 mM of ATCI, 50 μL of 50 mM Tris/HCl (pH = 8), 25 μL of enzyme, and 25 μL of three different concentrations (2.5, 7.5, and 15 μM) of inhibitor were added to the assay solution. Kinetic study of the hydrolysis of ATCI catalyzed by *EeAChE* was done spectrometrically at 405 nm every 11 s for 2 min and can be evaluated by the Michaelis–Menten model constructed by plotting velocity (V) opposite to the concentration of substrate (S) at varying concentrations of the substrate acetylthiocholine iodide (5, 10, 25, 50, 125, and 250 μM). Michaelis–Menten model was converted to Lineweaver–Burk model into a straight line by plotting $1/V$ velocity opposite to $1/S$ by Prism5 program. The type of inhibition (competitive, noncompetitive, uncompetitive, and mixed-type inhibition) can be determined from the variation of K_m and V_{max} at different inhibitor concentrations.

Cytotoxicity

The cytotoxicity assay of chromone derivatives against SH-SY5Y cells was measured using a sulforhodamine B (SRB) assay. Human neuroblastoma cell line SH-SY5Y (ATCC –2266) was purchased from ATCC. This cell line is the most appropriate *in vitro* model for therapeutic testing of neurodegenerative diseases (Xie et al. 2010). SH-SY5Y cells were cultured in DMEM: F12 supplemented with 10%

fetal bovine serum (Gibco, USA) and grown at 37 °C in a humid atmosphere containing 5% CO₂. Cells (8 × 10³ cells/well) were seeded in a 96-well plate and incubated at 37 °C, 5% CO₂ for 24 h. The cells were then treated with or without various concentrations (0, 0.4, 0.8, 1.5, 3.125, 6.25, 12.5, 25, 50 μM) of each compound for 48 h. After an incubation period, 40% (w/v) Trichloroacetic acid (TCA) was added to the cells and the cells were then incubated at 4 °C for 1 h. The medium was removed and the cells were rinsed with slow running tap water. 0.4% (w/v) SRB solution (100 μL) was added to each well and the cells were incubated for 1 h at room temperature. The SRB solution was removed and then the cells were washed 3 times with 1% (v/v) acetic acid and were allowed to dry at room temperature. The protein-bound dye was dissolved with 10 mM Tris base solution and the absorbance was measured at 492 nm using a microplate reader.

Neuroprotective studies against H₂O₂-induced stress

The SH-SY5Y cells were seeded into 96-well plates (8 × 10³ cells/well) and allowed to adhere for 24 h. Cells were then pretreated with 5 μM of the tested compound, and then freshly prepared H₂O₂ (from 30 % stock) was added at a concentration of 100 μM and further cultured for 24 h. To examine potential effects, the medium was removed following treatments, and the SRB assay was performed.

Molecular docking

In this study, AutoDock Vina 1.1.2 (Trott and Olson 2010); (Forli et al. 2016) and Discovery Studio 2.5 programs were used for molecular docking and visualization. The protocol included three main steps: the optimization of compounds, the minimization of enzymes and the molecular docking study to predict the structures of enzyme-ligand complexes (Lee 2008). The best compound from results of inhibitory activity was selected for this docking experiment. The structure of the compound was optimized using density functional theory at B3LYP/6-311 G (d, p) level while the enzymes were minimized using AMBER software. The protein was prepared under the protein preparation protocol achieved in Discovery Studio 2.5. PROKA was used to assign protonation state at neutral pH (pH = 7). The enzyme structures from *Torpedo californica* acetylcholinesterase (*TcAChE*, PDB ID: 1EVE) and human butyrylcholinesterase (*HuBChE*, PDB ID: 4BDS) were achieved from protein data bank (PDB) and the molecular docking studies were carried out where the binding site covered the PAS and CAS of the enzyme. The grid box center was set at the center of the active site of enzyme. For *TcAChE*, the center of the grid box was placed at the bottom of the active site gorge (x = 2.023, y = 63.295, z = 67.062), and the dimensions of the active site box were set at 50 Å ×

50 Å × 50 Å. For *HuBChE*, the center of the grid box was determined at x = 135.117, y = 119.222, z = 40.667, and the dimensions of the active site box were set at 34 Å × 46 Å × 34 Å. After that, ligands are put in the grid box to calculate free energy of binding (ΔG). Ligands are arranged by the calculated ΔG value; lower ΔG values correspond to more desirable ligand binding, while higher ΔG values are less desirable (favorable) (Trott and Olson 2010). The docking score is the predicted binding affinity in kcal/mol. Finally, the complex structures were evaluated using Discovery Studio 2.5 program.

Results and discussion

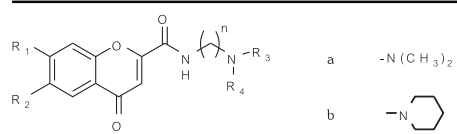
Chemistry

The chromone derivatives were prepared via 2-step synthesis. In the first step, ethyl-4-oxo-4*H*-chromene-2-carboxylate derivatives (4–6) were prepared from Claisen condensation (Walencyk et al. 2005) between 2-hydroxyacetophenone (1) or substituted 2-hydroxyacetophenone (2–3) and diethyl oxalate using sodium hydride as a base. The resulting esters were subjected to aminolysis (Bera et al. 2011) with *N*-alkyl dimethylamines or *N*-alkyl piperidine to yield the corresponding chromone derivatives (7–18, Scheme 1). Compounds 9 and 13 are known compounds (Walencyk et al. 2005) but the AChE inhibitory activity of these compounds has not been reported. Structure of the synthesized compounds was characterized with IR, ¹H-NMR, ¹³C-NMR and Mass spectrometry. The target compounds were successfully synthesized in high yield. Spectroscopic data and high-resolution mass spectrometry confirmed that the desired products were obtained.

In vitro inhibitory activity against AChE and BChE

In vitro AChE and BChE inhibitory activities were screened with electric eel AChE (*eeAChE*) and equine BChE enzymes using the colorimetric Ellman's method. All compounds exhibited potent acetylcholinesterase inhibitory activity with IC₅₀ values in micromolar level and showed moderate BChE inhibitory activities. Ellman's assay was further performed with *HuAChE* in order to infer acetylcholinesterase inhibitory activity of the compounds in human (Table 1).

From the Ellman's assay using *eeAChE*, compounds with unsubstituted chromone moiety (7–10) showed activities with IC₅₀ values ranging from 1.75 to 2.55 μM. Compound 8 (IC₅₀ = 1.75 ± 0.19 μM) was the most potent compound in this series. Compounds with 7-methoxyl chromone moiety (11–14, R₁ = OCH₃) showed activities with IC₅₀ values between 0.09–9.16 μM. Compound 14 (IC₅₀ = 0.09 ± 0.0003 μM) exerted the highest potency in this series and

Table 1 Inhibition concentration at 50% to AChE and BChE of chromone derivatives


Cpd	R ₁	R ₂	NR ₃ R ₄	n	IC ₅₀ ± SD (μM)			SI ^a
					<i>ee</i> AChE	<i>Hu</i> AChE	BChE	
7	H	H	a	2	7.58 ± 0.91	4.10 ± 0.66	22.95 ± 0.04	3.03
8	H	H	b	2	1.75 ± 0.19	6.38 ± 0.67	28.32 ± 1.60	16.18
9	H	H	a	3	3.42 ± 0.32	5.34 ± 0.43	14.51 ± 0.45	4.24
10	H	H	b	3	2.55 ± 0.06	1.61 ± 0.12	13.74 ± 0.96	5.38
11	OCH ₃	H	a	2	1.05 ± 0.22	2.15 ± 0.16	17.82 ± 0.92	16.97
12	OCH ₃	H	b	2	0.88 ± 0.08	1.73 ± 0.07	12.23 ± 0.76	13.89
13	OCH ₃	H	a	3	9.16 ± 0.24	3.16 ± 0.06	13.72 ± 0.48	1.49
14	OCH ₃	H	b	3	0.09 ± 0.0003	0.09 ± 0.02	27.91 ± 0.34	310.11
15	OCH ₃	OCH ₃	a	2	0.14 ± 0.03	2.78 ± 0.46	44.56 ± 0.46	318.29
16	OCH ₃	OCH ₃	b	2	0.41 ± 0.04	1.35 ± 0.07	39.62 ± 0.06	96.63
17	OCH ₃	OCH ₃	a	3	2.56 ± 0.06	3.15 ± 0.49	12.09 ± 1.23	4.72
18	OCH ₃	OCH ₃	b	3	0.78 ± 0.04	0.22 ± 0.02	32.3 ± 1.13	41.41
Tacrine					0.13 ± 0.02	0.31 ± 0.02	0.01 ± 0.001	0.86
Donepezil					0.006 ± 0.001	0.004 ± 0.001	1.06 ± 0.02	176.67

$$^a\text{SI} = (\text{IC}_{50} \text{ Horse BChE}) / (\text{IC}_{50} \text{ eeAChE})$$

among all synthesized compounds in this work. Compounds with 6,7-dimethoxyl chromone moiety (**15–18**, R₁ = R₂ = OCH₃) showed activities with IC₅₀ values in the range of 0.14–2.56 μM. Compound **15** (IC₅₀ = 0.14 ± 0.03 μM) exerted the best activity among compounds in this series.

Changing the amino group moiety from *N,N*-dimethyl group to piperidine ring generally resulted in higher potency. For example, in the unsubstituted chromones (**7–10**) with the same methylene chain length, **8** (n = 2, IC₅₀ 1.75 ± 0.19 μM) showed higher potency than **7** (n = 2, IC₅₀ 7.58 ± 0.91 μM). This trend was also observed among most compounds in the 7-methoxyl and 6,7-dimethoxyl chromone series. However, effect from varying the length of the methylene chain joining the chromone and amine moiety to AChE activity was not observed. From these findings, compound **14** (IC₅₀ = 0.09 ± 0.0003 μM) with 7-methoxyl chromone moiety and piperidine moiety was the most potent compound among the whole series. A similar trend was observed when the compounds were tested using human AChE. Compound **14** (IC₅₀ = 0.09 ± 0.02 μM) was still the most potent acetylcholinesterase inhibitor in this series. This supported the idea that compound **14** showed high potential for development for the treatment of AD in human. Most of the synthesized chromone derivatives were found to be moderately or non-selective to AChE. In contrast, compounds **14** (SI = 310.11) and **15** (SI = 318.29) were highly selective to AChE, almost two times more selective than donepezil (SI = 176.67), the dual-binding site inhibitor. Molecular docking was used to suggest insights in difference of binding energy and binding interaction between the compounds with AChE and BChE that led to the high selectivity to AChE.

Kinetic study

A kinetic study was carried out on the most potent compound in the series (**14**) with AChE from electric eel at three different concentrations (2.5, 7.5 and 15 μM) of the inhibitor. Lineweaver–Burk plot (Fig. 2) showed a decrease in V_{max} and K_m as the concentration of the inhibitor increased, which showed uncompetitive inhibition.

Compound **14** demonstrated uncompetitive inhibition to AChE. This mode of inhibition is different from donepezil which was indicated as a mixed-type AChE inhibitor. The mixed-type inhibitors were proposed to be able to bind with both the CAS and the PAS of the enzyme (8, 14). *N*-benzyl moiety in the structure of donepezil might facilitate binding at the CAS via π–π interaction resulting in dual-binding site inhibition. The uncompetitive inhibitor binds only with enzyme-substrate [ES] complex and gives enzyme-substrate-inhibitor [ESI] complex without binding to the free enzyme. Compound **14**, lack of *N*-benzyl group, might bind with the CAS with less affinity than donepezil. The smaller piperidine moiety of **14** might allow larger room at the bottom of the active site gorge for substrate binding, then **14** might bind with the [ES] complex to give enzyme-substrate [ES] complex and thus block the action of AChE.

Cytotoxicity and neuroprotective effect studies

To gain insight into the therapeutic potential of synthesized compounds, the cytotoxicity and neuroprotective capacity against oxidative stress were investigated in the human SH-SY5Y neuroblastoma cell line. First, we examined the cytotoxic effects of the selected compounds, including **10**,

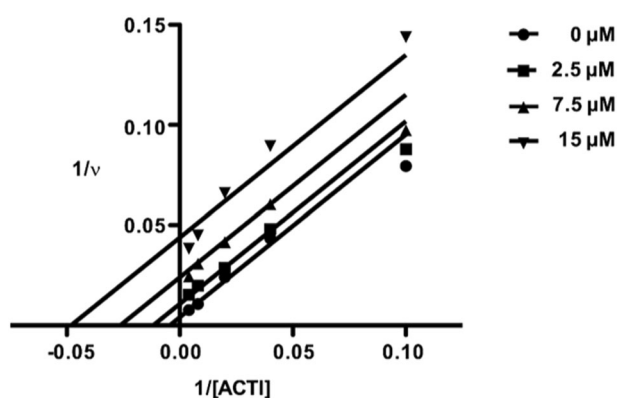


Fig. 2 Lineweaver–Burk plot illustrating uncompetitive types of *ee*AChE inhibition for compound **14**. The inverse initial velocity (V^{-1}) as a function of the inverse of the substrate concentration ($[ACTI]^{-1}$) was plotted for different concentrations of inhibitor (0.0, 2.5, 7.5 and 15 μM)

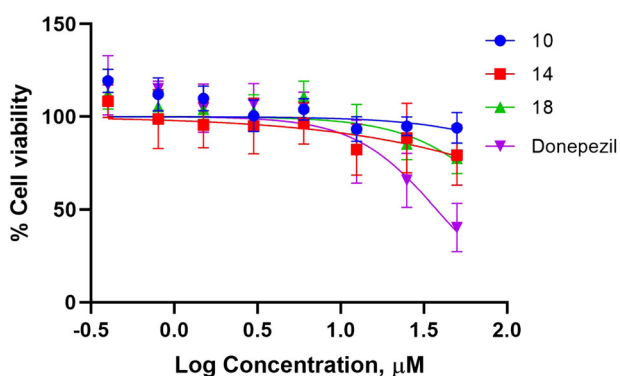


Fig. 3 Cytotoxic effect of synthesized compounds on SH-SY5Y cells as determined by SRB assay. Cells were treated with the synthesized compounds at different concentrations for 48 h, and then SRB assay was performed. Data are means \pm SD of three independent experiments and %cell viability was calculated relative to nontreated control

14, **18**, on the cell viability of SH-SY5Y cells by using SRB assay. The cells were treated with varying concentrations ranging from 0.4 to 50 μM of the tested compounds for 48 h. As shown in Fig. 3, results revealed that all of the test compounds did not show significant toxicity at any tested concentrations to the neuron cells ($LC_{50} > 50 \mu\text{M}$) when compared with the reference compound, donepezil, ($LC_{50} = 43.13 \pm 7.9 \mu\text{M}$). This result suggested safety of the chromone derivatives when used with the neuronal cell line at the effective lower micromolar level.

Oxidative stress plays an important role in the progression of AD. Therefore, in this study, we also investigated the neuroprotective effect against H_2O_2 -induced cell death of chromone derivatives. Exposure of cells to 100 μM H_2O_2 induced significant oxidative stress leading to the reduction of cell viability, $\sim 20\%$ of control after 24 h exposure (Fig. 4). In order to test the neuroprotective effect of selected chromone series, cells were pretreated with 5 μM of

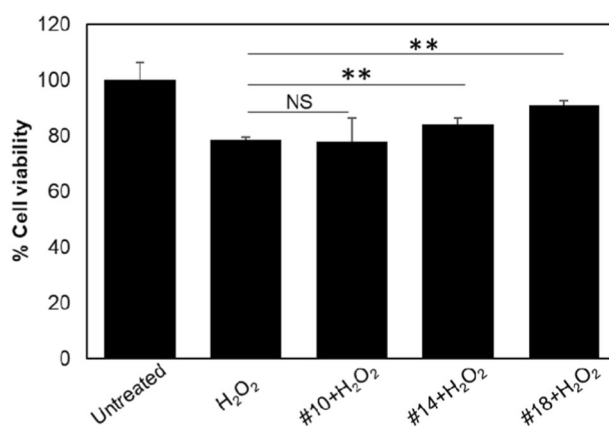


Fig. 4 Neuroprotective effect of synthesized compounds on H_2O_2 -induced cytotoxicity in SH-SY5Y cells. Cells were pretreated with 5 μM of the tested compound for 24 h and then 100 μM of freshly prepared H_2O_2 was added and further cultured for 24 h. Cell viability was determined by SRB assay. Data are means \pm SD of three independent experiments and %cell viability was calculated relative to nontreated control; $**p < 0.05$

the tested compound followed by exposure to 100 μM H_2O_2 . The result showed that among all the compounds, **14** and **18** exhibited neuroprotective activities against H_2O_2 -induced damage at 5 μM , restoring cell viability at 7.1% and 15.5%, respectively. This result suggested effectiveness of compounds **14** and **18** in preventing oxidative stress to neuronal cells. Compounds **14** and **18** showed neuroprotective effects against H_2O_2 -induced cell death. The methoxyl substituent(s) may play a role in the anti-oxidative effect of the compounds.

Molecular docking

The most potent chromone-2-carboxamido-alkylamine derivative (**14**) was further studied for binding interactions and binding affinity using molecular docking. Compound **14** showed selectivity to AChE ($SI = 310.11$) that is approximately two times higher than donepezil ($SI = 176.67$, Table 1). In order to explain this high selectivity of **14** over donepezil, binding affinity with AChE and BChE enzymes of the two molecules were compared.

The initial structures of *Tc*AChE and *Hu*BChE were retrieved from protein data bank with PDB ID: 1EVE and 4BDS, respectively. A molecular modeling study was performed using the docking program by AutoDock Vina 1.1.2 and Discovery studio 2.5. The result showed affinity of binding energy between the enzyme and the compound as noted in Table 2. The molecular docking studies of compound **14** and donepezil resulted in the low-negative binding energy which indicated strong favorable binding for both enzymes (*Tc*AChE and *Hu*BChE). The lowest binding energy conformer of each ligand was selected to investigate the residue interaction. Furthermore, distance values which

measured the distance between amino acid residues in the active sites of enzyme and functional groups on the ligands were calculated and illustrated in Fig. 5.

Compound **14**-*TcAChE* complex showed affinity of binding energy of -9.5 kcal/mol (Table 2). Compound **14** occupied the entire enzymatic PAS, mid-gorge, and CAS

Table 2 Binding energy of the chromone derivative in comparison with donepezil

Compound	IC ₅₀ ± SD (μM)			Binding energy (kcal/mol)	
	<i>EeAChE</i>	<i>Horse BChE</i>	<i>HuAChE</i>	<i>TcAChE</i>	<i>HuBChE</i>
14	0.09 ± 0.0003	27.91 ± 0.34	0.09 ± 0.02	-9.5	-7.9
Donepezil	0.006 ± 0.001	1.06 ± 0.02	0.004 ± 0.001	-10.9	-9.1

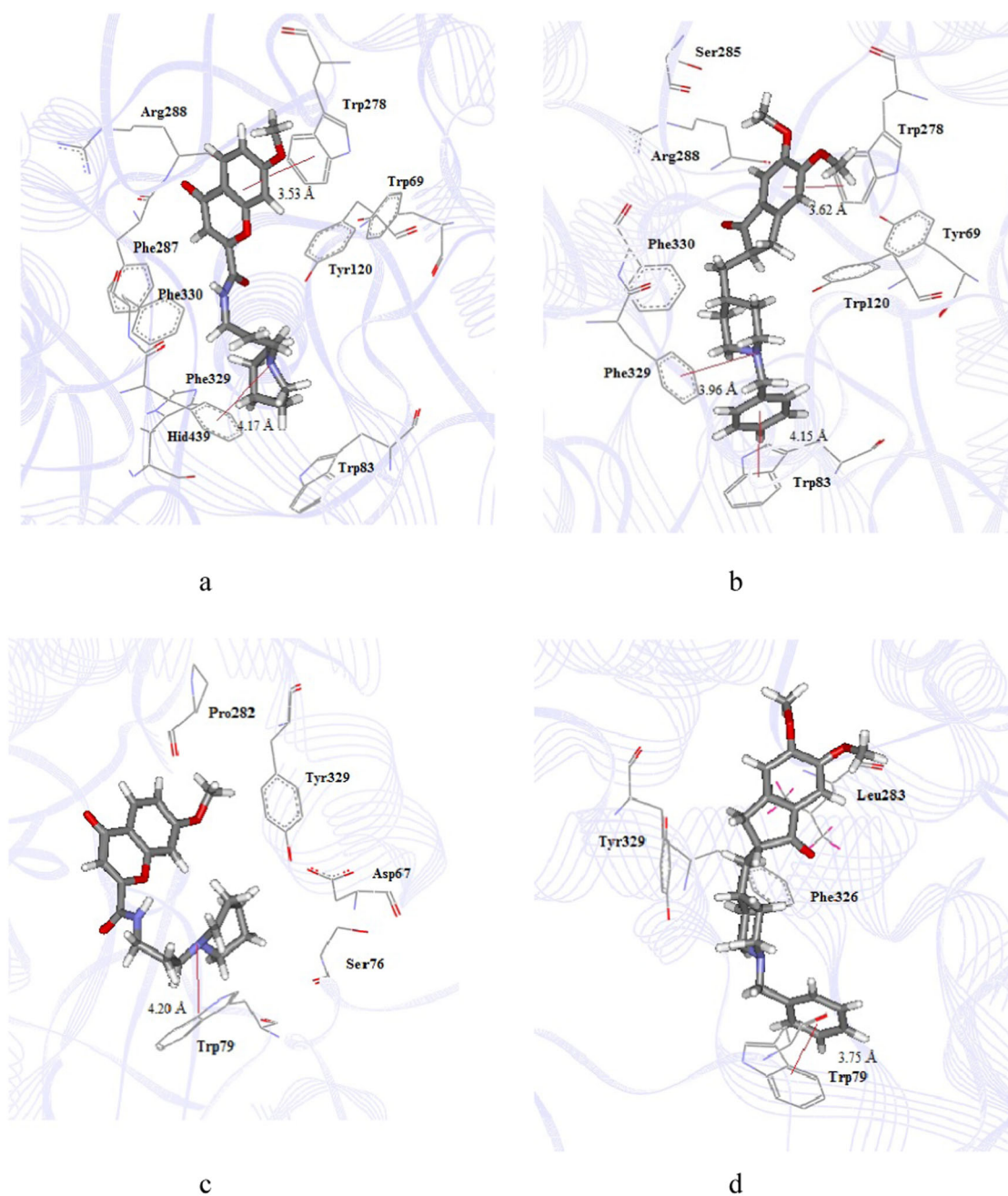


Fig. 5 Molecular docking study of **14**-*TcAChE* (a), Donepezil-*TcAChE* (b), **14**-*HuBChE* (c), and Donepezil-*HuBChE* (d) complexes

regions (Fig. 5a). The chromone moiety showed interaction with PAS of active site of enzyme and showed π - π interaction with Trp278 (distance of 3.53 Å), methylene chain showed hydrophobic interaction with Phe330 in the mid-gorge and piperidine ring of compound showed cation- π interaction with Phe329 (distance of 4.17 Å).

In **14**-*Hu*BChE complex, the affinity of binding energy was calculated as -7.9 kcal/mol (Table 2) demonstrating weak affinity to BChE. The tertiary amino group of the compound interacted only with Trp79 (distance of 4.20 Å) with cation- π interaction (Fig. 5c). These findings might reflect the higher selectivity of **14** toward AChE over BChE. Donepezil-*Tc*AChE (Fig. 5b) complex showed the binding affinity of -10.9 kcal/mol. Strong interactions between donepezil and the enzyme were observed in several areas of the active site gorge. The indanone ring of donepezil was observed to bind to the PAS via a π - π interaction with Trp278 at the distance of 3.62 Å. The long chain of methylene was observed to bind to the mid-gorge via a hydrophobic interaction with Phe330. The piperidine ring was observed to bind to the CAS via a cation- π interaction with Phe329 at the distance of 3.96 Å. The benzyl group of donepezil additionally interacted with Trp83 at the bottom of the gorge by π - π interaction at the distance of 4.15 Å. This might facilitate affinity of the drug to the active site gorge, both at the PAS and CAS sites, and explain the higher potency in AChE inhibition and the mixed-type inhibition of donepezil. On the other hand, compound **14** could bind at an upper part of the CAS and allow some space for substrate binding at the bottom of the gorge. This might allow the compound to bind with (ES) complex and explain uncompetitive inhibition of **14**.

In donepezil-*Hu*BChE complex (Fig. 5d), the binding energy affinity of -9.1 kcal/mol was observed. This complex exhibited hydrophobic interaction with Tyr329 at mid-gorge of active site and π - π interaction between the benzyl group and Trp79 at the distance of 3.75 Å. From these results, donepezil binds to AChE and BChE with high affinity (more negative binding energy), while **14** showed lower energy and a larger difference in binding energy values between both enzymes. These findings corresponded well with the higher selectivity toward AChE of **14**.

Conclusions

Twelve novel chromone-2-carboxamido-alkylamines were designed, synthesized and evaluated for their acetyl- and butyrylcholinesterase inhibitory activities. All compounds in this series exhibited potent acetylcholinesterase inhibitory activity in micro- to nanomolar ranges. Compound **14** was the most potent AChE inhibitor with IC_{50} value $0.09 \pm 0.0003 \mu\text{M}$

and showed high selectivity to AChE (SI = 310.11). Kinetic study suggested that **14** is an uncompetitive AChE inhibitor. Results from molecular docking supported the enzyme inhibitory results and high selectivity to AChE of the compound. As proposed, the chromone nucleus showed affinity to the PAS of AChE and the piperidine nitrogen showed affinity with the CAS of the enzyme. Cytotoxicity of the chromone derivatives was further determined in SH-SY5Y cell line and the compounds showed higher cell viability than donepezil at the same concentration. The selected chromone-2-carboxamido-alkylamines demonstrated a neuroprotective effect. These findings supported that chromone derivatives are promising for further evaluation and development as agents for the treatment of AD.

Acknowledgements We would like to thank Prince of Songkla University (Grant No. PHA590412S) and the University of Malaya (UMRG: RP037D-17AFR) for financial support of this study. The authors would like to thank Miss Maria Mullet for providing linguistic proofreading for the manuscript.

Compliance with ethical standards

Conflict of interest The authors declare that they have no conflict of interest.

Publisher's note Springer Nature remains neutral with regard to jurisdictional claims in published maps and institutional affiliations.

References

- Ahmed M, Rocha JB, Corrêa M, Mazzanti CM, Zanin RF, Morsch AL, Morsch VM, Schetinger MR (2006) Inhibition of two different cholinesterases by tacrine. *Chem Biol Interact* 162: 165–171
- Baptista FI, Henriques AG, Silva AM, Wiltfang J, da Cruz e Silva OA (2014) Flavonoids as therapeutic compounds targeting key proteins involved in Alzheimer's disease. *ACS Chem Neurosci* 5:83–92
- Bera K, Sarkar S, Biswas S, Maiti S, Jana U (2011) Iron-catalyzed synthesis of functionalized 2H-chromenes via intramolecular alkyne-carbonyl metathesis. *J Org Chem* 76:3539–3544
- Bourne Y, Taylor P, Marchot P (1995) Acetylcholinesterase inhibition by fasciculins: crystal structure of the complex. *Cell* 83:503–512
- Castro A, Martinez A (2001) Peripheral and dual binding site acetylcholinesterase inhibitors: implications in treatment of Alzheimer's disease. *Mini Rev Med Chem* 1:267–272
- Chatonnet A, Lockridge O (1989) Comparison of butyrylcholinesterase and acetylcholinesterase. *Biochem J* 260:625–634
- Cokugras AN (2003) Butyrylcholinesterase: structure and physiological importance. *Turk J Biochem* 28:54–61
- Ellman GL, Courtney KD, Andres Jr V, Featherstone RM (1961) A new and rapid colorimetric determination of acetylcholinesterase activity. *Biochem Pharm* 7:88–95
- Forli S, Huey R, Pique ME (2016) Computational protein-ligand docking and virtual drug screening with the AutoDock suite. *Nat Protoc* 11:905–919
- Grazul M, Budzisz E (2009) Biological activity of metal ions complexes of chromones, coumarins and flavones. *Coord Chem Rev* 253:2588–2598

- Greenblatt HM, Kryger G, Lewis T, Silman I, Sussman JL (1999) Structure of acetylcholinesterase complexed with (-)-galanthamine at 2.3 Å resolution. *FEBS Lett* 463:321–326
- Greig NH, Lahiri DK, Sambamurti K (2002) Butyrylcholinesterase: an important new target in Alzheimer's disease therapy. *Int Psychogeriatr* 14:77–91
- Hardy J, Selkoe JD (2002) The amyloid hypothesis of Alzheimer's disease: progress and problems on the road to therapeutics. *Science* 297:353–356
- Kamal MA, Greig NH, Alhomida AS, Al-Jafari AA (2000) Kinetics of human acetylcholinesterase inhibition by the novel experimental Alzheimer therapeutic agent, tolserine. *Biochem Pharm* 60:561–570
- Lee K (2008) Computational study for protein-protein docking using global optimization and empirical potentials. *Int J Mol Sci* 9:65–77
- Liston DR, Nielsen JA, Villalobos A, Chapin D, Jones SB, Hubbard ST, Shalaby IA, Ramirez A, Nason D, White WF (2004) Pharmacology of selective acetylcholinesterase inhibitors: implications for use in Alzheimer's disease. *Eur J Pharm* 486:9–17
- Liu Q, Qiang X, Li Y, Sang Z, Li Y, Tan Z, Deng Y (2015) Design, synthesis and evaluation of chromone-2-carboxamidoalkylbenzylamines as multifunctional agents for the treatment of Alzheimer's disease. *Bioorg Med Chem* 23:911–923
- Luo W, Chen Y, Wang T, Hong C, Chang LP, Chang CC, Yang YC, Xie SQ, Wang CJ (2016) Design, synthesis and evaluation of novel 7-aminoalkyl-substituted flavonoid derivatives with improved cholinesterase inhibitory activities. *Bioorg Med Chem* 24:672–680
- Mayeux R, Sano M (1999) Treatment of Alzheimer's disease. *N Engl J Med* 341:1670–1679
- Mehta M, Adem A, Sabbagh M (2012) New acetylcholinesterase inhibitors for Alzheimer's disease. *Int J Alzheimers Dis* 2012:1–8
- Nochi S, Asakawa N, Sato T (1995) Kinetic study on the inhibition of acetylcholinesterase by 1-benzyl-4-[(5,6-dimethoxy-1-indanon-2-yl)methyl]piperidinehydrochloride (E2020). *Biol Pharm Bull* 18:1145–1147
- Pourshojaei Y, Gouranourimi A, Hekmat S, Asadipour A, Rahmani-Nezhad S, Moradi A, Nadri H, Moghadam FH, Emami S, Foroumadi A, Shafiee (2015) A Design, synthesis and anticholinesterase activity of novel benzyldenechroman-4-ones bearing cyclic amine side chain. *Eur J Med Chem* 97:181–189
- Rogers SL, Friedhoff LT (1998) Long-term efficacy and safety of donepezil in the treatment of Alzheimer's disease: an interim analysis of the results of a US multicentre open label extension study. *Eur Neuropsychopharmacol* 8:67–75
- Sang Z, Qiang X, Li Y, Xu R, Cao Z, Song Q, Wang T, Zhang X, Liu H, Tan Z, Deng Y (2017) Design, synthesis and evaluation of scutellarein-O-acetamidoalkylbenzylamines as potential multifunctional agents for the treatment of Alzheimer's disease. *Eur J Med Chem* 28:307–323
- Sugimoto H, Yamanishi Y, Iimura Y, Kawakami Y (2000) Donepezil hydrochloride (E2020) and other acetylcholinesterase inhibitors. *Curr Med Chem* 7:303–339
- Tang BL, Kumar R (2008) Biomarkers of mild cognitive impairment and Alzheimer's disease. *Ann Acad Med Singap* 37:406–410
- Trott O, Olson AJ (2010) AutoDock Vina: improving the speed and accuracy of docking with a new scoring function, efficient optimization and multithreading. *J Comput Chem* 31:455–461
- Walencyk T, Carola C, Buchholz H, König B (2005) Chromone derivatives which bind to human hair. *Tetrahedron* 61:7366–7377
- Xie HR, Hu LS, Li GY (2010) SH-SY5Y human neuroblastoma cell line: In vitro cell model of dopaminergic neurons in Parkinson's disease. *Chin Med J* 123:1086–1092
- Yiannopoulou KG, Papageorgiou SG (2013) Current and future treatments for Alzheimer's disease. *Ther Adv Neurol Disord* 6:19–33